

Scaling and universality in two dimensions: three-body bound states with short-ranged interactions

F F Bellotti¹, T Frederico¹, M T Yamashita², D V Fedorov³, A S Jensen³ and N T Zinner³

¹Instituto Tecnológico de Aeronáutica, DCTA, 12.228-900 São José dos Campos, SP, Brazil

²Instituto de Física Teórica, UNESP - Univ Estadual Paulista, C.P. 70532-2, CEP 01156-970, São Paulo, SP, Brazil

³Department of Physics and Astronomy - Aarhus University, Ny Munkegade, bygn. 1520, DK-8000 Århus C, Denmark

Abstract. The momentum space zero-range model is used to investigate universal properties of three interacting particles confined to two dimensions. The pertinent equations are first formulated for a system of two identical and one distinct particle and the two different two-body subsystems are characterized by two-body energies and masses. The three-body energy in units of one of the two-body energies is a universal function of the other two-body energy and the mass ratio. We derive convenient analytical formulae for calculations of the three-body energy as function of these two independent parameters and exhibit the results as universal curves. In particular, we show that the three-body system can have any number of stable bound states. When the mass ratio of the distinct to identical particles is greater than 0.22 we find that at most two stable bound states exist, while for two heavy and one light mass an increasing number of bound states is possible. The specific number of stable bound states depends on the ratio of two-body bound state energies and on the mass ratio and we map out an energy-mass phase-diagram of the number of stable bound states. Realizable systems of both fermions and bosons are discussed in this framework.

PACS numbers: 03.65.Ge,68.65.-k,67.85.-d,21.45.-v

1. Introduction

Quantum mechanics in two-dimensional (2D) systems differs quite markedly from the three-dimensional (3D) case in many aspects. A particular example is the centrifugal barrier which is zero or positive in 3D, whereas in 2D the s -wave barrier is in fact negative. This implies that two particles in 2D are at the threshold of binding even when they do not interact, i.e. an infinitesimal attraction will produce a bound state [1, 2, 3]. This is seen in the famous Landau criterion which says that potentials with negative volume integral will produce a bound state for any value of the strength [4]. In fact, even when the volume integral is exactly zero a bound state is still present [5, 6, 7, 8, 9, 10]. These results are in sharp contrast to the 3D arena where it is well-known that a finite amount of attraction is required to produce bound states.

A natural question to ask is how these dimensional differences influence few-body states with more than two particles. A direction of research has therefore been to derive and establish conditions for the occurrence of properties of such systems. Most prominent among the findings is arguably the Efimov effect [11] which has achieved a unique position as a mathematical anomaly of three interacting particles in 3D. The so-called Efimov states generally correspond to excited states that reside at large distance and owe their properties to large two-body scattering lengths. The relative properties, however, do not even depend on the scattering length but only on the mass ratios of the constituent particles which determine for instance the scaling of energy and size from one state to the next. These scalings are completely independent of the short-distance details of the inter-particle potentials.

A number of universal relations have been found and studied in 3D. The classical examples are correlations between two observables where a one-dimensional relation emerges when the potentials are varied. The Phillips plot is one curve for different potentials when the neutron-deuteron scattering length is plotted versus the triton binding energy [12], the Coester line of saturation density versus binding energy per nucleon for nuclear matter [13], and the Tjon line is the correlation between binding energies of three and four nucleons [14]. Other much more abundant 3D systems with very little model dependence have been found and baptized halo systems [15]. They were at first primarily found as states in nuclei but quickly they were also search for in molecules, and in particular as helium dimers and trimers [16]. Universal relations have been applied to check for Efimov excited states in nuclear halo systems [17] and also in molecules [18].

The study of the Efimov effect has seen a revival in recent years within the context of ultracold atomic gases after its initial observation in a gas of Cesium atoms in 2006 [19]. This was followed by a number of experiments using various atomic species and a new subfield dubbed 'Efimov Physics' has since developed (see the recent review in Ref. [20]). Some of the latest experiments have demonstrated heteronuclear Efimov states [21] and also the presence of some intriguing four-body states [22, 23, 24] tied to the Efimov trimers [25, 26].

Common to all the studies and experiments mentioned thus far is that they are 3D. If one considers instead a 2D setup, then the structure of the three-body states is very different. In the case of three equal mass particles the tower of states close to threshold is absent and one finds just two bound states in the universal limit where the particles reside outside the range of the two-body potential [1, 27]. Here we investigate a system of three particles where two are assumed identical as function of the two-body interaction energies and the mass ratios. As we will demonstrate, one can potentially have any number of stable bound states when the parameters of the system are varied. We therefore find a much more varied picture of 2D three-body systems in the universal limit than has previously been considered.

Two-dimensional physics is important for a variety of problems such as high-temperature superconductors, localization of atoms on surfaces, in semiconducting microcavities, and for carbon nanotubes and organic interfaces. One particular interesting example is the two-component Fermi gas with attractive interactions in 2D. Here the pairing instability is caused by the presence of a two-body bound *s*-wave state [28, 29, 30]. The role of three-body states, however, remains elusive. In the ultracold atomic gas community there is great interest in producing quantum degenerate gases in low dimensions to investigate some of the basic features of a 2D environment. Early experiments succeeded in producing quasi-2D samples of ^{133}Cs [31, 32, 33], ^{23}Na [34], and ^{87}Rb [35]. Mixtures of ^{40}K and ^{87}Rb have been used to produce 2D gases [36, 37], and more recently samples with two-component gases of ^6Li [38, 39] and ^{40}K [40] have been studied. Heteronuclear molecules $^{40}\text{K}^{87}\text{Rb}$ have also been trapped in a layered stack of quasi-2D pancakes [41].

Quasi-2D system are abundant in ultracold atom physics and we thus expect that our predictions can be studied in a variety of these setups. In a real experiment the confinement to 2D is typically done using an optical lattice. This introduces a transverse energy scale, $\hbar\omega_0$. Below this scale the physics is effectively 2D while it becomes 3D at or above $\hbar\omega_0$. In this first study we will assume a strict 2D setup, which amounts to assuming that we are always working far below $\hbar\omega_0$. In some of the limiting cases considered here this assumption breaks down and in those cases the trap must be explicitly included to make predictions for real experiments. However, in the weak-coupling limit where the two-body bound state energies of all three subsystems is small we expect our results to apply directly. The two-body energy must, however, be modified to include the trap scale in the manner outlined in Ref. [42]. In addition, confinement-induced resonances occur in low-dimensional systems [43] and have to be taken into account when considering the possible few-body bound states. We expect that techniques for detection of three-body states and resonances in 3D will also be useful in the quasi-2D case, i.e. identification of sharp features in the loss rates [20] or radio-frequency association [44, 45].

The three-body states we consider here consist of two identical particles and a third distinct particle. This can be a system consisting of two identical bosons and a third particle, or two fermions with at least two internal degrees of freedom (typically

hyperfine projections in the case of ultracold alkali gases). As we consider the s -wave channel only in our equations, this means that in the case of two identical fermions, the interaction is necessarily zero. While there could be interaction in higher partial waves, we neglect these in the present study as they are usually much smaller than the s -wave interactions.

We illustrate the generic system under consideration in figure 1a) as a plane with two identical A particles and one B particle. The plane is drawn as a pancake which is the typical experimental situation. In the picture we assume that the mass of A is smaller than that of B but we will consider both cases below. In figure 1b) we show another interesting setup for which our results are relevant, a multi-layer stack of pancakes with particles of both kind in each of the layers. In addition to the in-plane three-body states that are possible, a long-range force that acts across the layers can also provide binding. Our results are then relevant in the universal limit which applies for ultracold polar molecules with small dipole moments. This has been discussed in one- [46] and three-dimensional systems very recently [47], and for the 2D bi- and multi-layers in the weak [6, 7, 8, 9, 10] and strongly coupled cases [48]. This 2D multi-layer with dipolar particles has been experimentally realized as mentioned above [41].

Occurrence conditions and properties of model independent or universal states, like in Efimov or halo physics [49], are studied using zero-range models where the properties of the systems arise from distances larger than the interaction ranges [50, 51]. The behavior is important as a measure against such asymptotic properties, but clearly also directly if these properties can be realized in Nature or in laboratories. Both these roles now appear more and more in 2D physics. The purpose of the present paper is to provide universal energy relations for three-body systems in 2D. These relations are completely general and specific applications only require appropriate two-body input parameters.

The structure of the paper is as follows. The introduction is followed by a sketch in section II of the method. Equipped with the appropriate equations the numerical investigations follow in section III. The stability of ground and excited states are studied in section IV. Along the way we reformulate the integral equation to apply to various threshold properties. In section V we briefly sum up and formulate the conclusions.

2. Formalism and Notation

We consider a two-dimensional AAB system assuming that the interactions depend only on relative distances. This can be a three-body system in a single plane as in figure 1a) or three particles in two or three layers when long-range interactions are present as in figure 1b). In both situations, the three-particle dynamics effectively happens in a single plane. We use zero-range interactions as we are interesting in the for model-independent universal limit. This simplifies the formulation of the Faddeev equation for the three-body bound state as the contact interaction is separable. In the case of long-range interaction across different layers, the use of zero-range interactions assumes that the

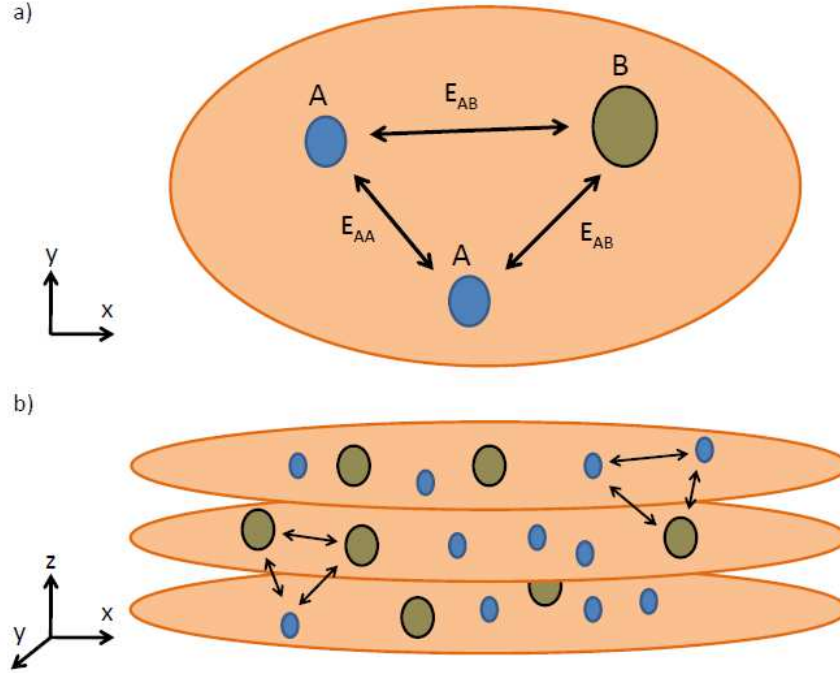


Figure 1. Schematic illustration of the generic setup considered. a) A three-body system in a plane (depicted more realistically as a pancake with ellipsoidal shape to indicate potential trap deformation) with two identical A particles and one B particle (top view). The picture indicates that the mass of B is larger than that of A. Two-body interaction energies, E_{AA} and E_{AB} , and coordinate axis are also shown. b) A multi-layer setup containing multiple A and B particles (side view). In a system with long-range interactions (like dipole-dipole forces) three-body states can be formed from particles in the same plane and in different planes. Two kinds of three-body systems with particles in adjacent layers are indicated by arrows. Coordinate system is shown on the left.

low-energy properties of the true long-range interaction can be described by an effective interaction of zero-range similarly to the van der Waals interaction for neutral atoms in 3D. This is true for potentials that go to zero at infinity faster than $1/r^2$ in 2D [52], which includes the dipolar $1/r^3$ interaction.

The 2D Hamiltonian for the three-particle AAB system with a pairwise potential is

$$H = H_0 + V_{AA} + V_{AB} + V_{AB} \quad (1)$$

where the two A particles are assumed to be identical bosons. The kinetic energy operator is

$$H_0 = \frac{\mathbf{q}_A^2}{2\mu_{A,AB}} + \frac{\mathbf{p}_A^2}{2\mu_{AB}} = \frac{\mathbf{q}_B^2}{2\mu_{B,AA}} + \frac{\mathbf{p}_B^2}{2\mu_{AA}} = \frac{\mathbf{q}_{A'}^2}{2\mu_{A,AB}} + \frac{\mathbf{p}_{A'}^2}{2\mu_{AB}}, \quad (2)$$

where we use Jacobi relative momenta given in terms of rest frame momenta, \mathbf{k}_i with

$i = \alpha, \beta, \gamma$, as

$$\mathbf{q}_\gamma = \mathbf{k}_\gamma \text{ and } \mathbf{p}_\gamma = \mu_{\alpha\beta} \left(\frac{\mathbf{k}_\alpha}{m_\alpha} - \frac{\mathbf{k}_\beta}{m_\beta} \right) \quad (3)$$

where (α, β, γ) is the cyclic permutations of the particles (A, A', B) with masses m_A and m_B . The reduced masses are $\mu_{\alpha\beta} = \frac{m_\alpha m_\beta}{m_\alpha + m_\beta}$ and $\mu_{\gamma, \alpha\beta} = \frac{m_\gamma(m_\alpha + m_\beta)}{m_\alpha + m_\beta + m_\gamma}$. The contact potential in operator form is

$$V_{\alpha\beta} = \lambda_{\alpha\beta} |\chi_{\alpha\beta}\rangle \langle \chi_{\alpha\beta}|, \quad (4)$$

where the form factor $\chi_{\alpha\beta}(\mathbf{p}_\gamma) = 1$, depends only on the relative momentum of the pair.

The two-body T-matrix for negative energies and zero-range potentials for AA and AB subsystems is

$$T_{A\gamma}(E) = |\chi_{A\gamma}\rangle \tau_{A\gamma}(E) \langle \chi_{A\gamma}|, \quad (5)$$

where, the matrix element of the 2D transition matrices are given by (see e.g. [50] for the case of identical particles)

$$\tau_{A\gamma}(E) = \left[-4\pi \frac{m_A m_\gamma}{m_A + m_\gamma} \ln \left(\sqrt{\frac{E}{E_{A\gamma}}} \right) \right]^{-1}, \quad (6)$$

where $\gamma = A$ or B and $E_{A\gamma}$ is the energy of the AA and AB two-body bound states. We adopt units such that $\hbar = 1$. The singularity of the two-body scattering equation in 2D is subtracted by fixing the pole at the two-body bound state (see e.g. [53]). To find the bound AAB system we concentrate on the negative energy region but note that for positive energy scattering, the analytic extension can be easily performed in (6). We note that effective range corrections have recently been discussed for three identical bosons [54] and will in general shift the binding energies. Such corrections can be included in the current formalism and can presumably be tuned in experiment by choosing different Feshbach resonances and trapping frequencies. However, since we are mainly interested in the overall structures (such as the number of bound states for given masses and interaction ratios) we neglect such corrections in this study.

The bound state wave function $|\Psi_{AAB}\rangle$ decomposed in terms of the Faddeev components is

$$|\Psi_{AAB}\rangle = |\Psi_A\rangle + |\Psi_{A'}\rangle + |\Psi_B\rangle \quad (7)$$

where $|\Psi_\gamma\rangle = G_0(E) V_{\alpha\beta} |\Psi_{AAB}\rangle$ with the resolvent $G_0(E) = (E - H_0)^{-1}$ which is nonsingular for bound states. The Faddeev equations are written in terms of the transition matrix, which is well defined for the zero range potential and given by (5). We then have

$$|\Psi_\gamma\rangle = G_0(E) T_{\alpha\beta} \left(E - \frac{\mathbf{q}_\gamma^2}{2\mu_{\gamma, \alpha\beta}} \right) (|\Psi_\alpha\rangle + |\Psi_\beta\rangle), \quad (8)$$

which simplifies through the separability of the potential to give

$$|\Psi_\gamma\rangle = G_0(E) |\chi_{\alpha\beta}\rangle |f_\gamma\rangle, \quad (9)$$

where $\langle \mathbf{q}_\gamma | f_\gamma \rangle = \lambda_{\alpha\beta} \langle \mathbf{q}_\gamma, \chi_{\alpha\beta} | \Psi_{AAB} \rangle$ is the vertex function of the Faddeev component of the wave function.

The coupled set of homogeneous integral equations for the Faddeev components of the vertices of the wave function for the bound AAB system follows from (8) and (9) and gives (see e.g. [50] and [51] for three identical bosons)

$$f_B(\mathbf{q}) = 2\tau_{AA} \left(E_3 - \frac{m_B + 2m_A}{4m_A m_B} \mathbf{q}^2 \right) \times \int d^2k \frac{f_A(\mathbf{k})}{E_3 - \frac{m_A + m_B}{2m_A m_B} \mathbf{q}^2 - \mathbf{k}^2 - \mathbf{k} \cdot \mathbf{q}}, \quad (10)$$

$$f_A(\mathbf{q}) = \tau_{AB} \left(E_3 - \frac{m_B + 2m_A}{2m_A(m_B + m_A)} \mathbf{q}^2 \right) \times \left[\int d^2k \frac{f_B(\mathbf{k})}{E_3 - \mathbf{q}^2 - \frac{m_A + m_B}{2m_A m_B} \mathbf{k}^2 - \mathbf{k} \cdot \mathbf{q}} + \int d^2k \frac{f_A(\mathbf{k})}{E_3 - \frac{m_A + m_B}{2m_A m_B} (\mathbf{q}^2 + \mathbf{k}^2) - \frac{m_A}{m_B} \mathbf{k} \cdot \mathbf{q}} \right], \quad (11)$$

where the AA and AB transition amplitudes are calculated for the energies of the corresponding subsystems through (8). We note that the coupled set of homogeneous equations described above gives the 3D equations for a bound system AAB when the transition amplitudes and momentum volume are conveniently substituted by their 3D forms [17].

The AAB wave function for the zero-range interaction is a solution of the 2D free Schrödinger equation except when the particles overlap. In momentum space, the wave function is built from the spectator functions, $f_A(\mathbf{q}_A)$ and $f_B(\mathbf{q}_B)$, which are solutions of the coupled equations (10) and (11). The relative Jacobi momentum of particle A with respect to the center of mass of AB is given by \mathbf{q}_A and for B with respect to AA by \mathbf{q}_B . The AAB wave function becomes

$$\Psi_{AAB}(\mathbf{q}_A, \mathbf{p}_A) = \frac{f_A(\mathbf{q}_A) + f_A(\mathbf{q}_{A'}) + f_B(\mathbf{q}_B)}{E_3 - \frac{2m_A + m_B}{2m_A(m_A + m_B)} \mathbf{q}_A^2 - \frac{m_A + m_B}{2m_A m_B} \mathbf{p}_A^2}, \quad (12)$$

where the relative Jacobi momenta \mathbf{q}_B and $\mathbf{q}_{A'}$ are combinations of the pair $(\mathbf{q}_A, \mathbf{p}_A)$ with \mathbf{p}_A the relative momentum between A and B defined in (3).

3. Universal properties

We want to find the s -wave three-body binding energy, E_3 , for a system of one distinct B particle and two identical A particles. This yields E_3 as function of the two masses, (m_A, m_B) , and the two-body binding energies, (E_{AA}, E_{AB}) . These four quantities are the only unknown parameters in the set of equations (10) and (11) which determine E_3 . Therefore E_3 must be a function of these four parameters. By using one of the binding energies, E_{AB} , as the unit of energy and m_A as the mass unit, we see from (10) and (11)

that the scaled three-body energy, ϵ_3 can be expressed in terms of only two independent dimensionless variables, that is

$$\epsilon_3 \equiv \frac{E_3}{E_{AB}} = \mathcal{F} \left(\frac{E_{AA}}{E_{AB}}, \frac{m_B}{m_A} \right) \equiv \mathcal{F}_n(\epsilon_{AA}, m), \quad (13)$$

where we used the definitions

$$m = \frac{m_B}{m_A}, \quad \epsilon_3 = \frac{E_3}{E_{AB}}, \quad \text{and} \quad \epsilon_{AA} = \frac{E_{AA}}{E_{AB}}. \quad (14)$$

The universal functions, \mathcal{F}_n , are distinctly different for ground and excited states as indicated by the discrete subscript n . We shall predominantly focus on the ground state ($n = 0$) but also extract information about the number of bound states for a given set of parameters. When the A particles are identical fermions, the interaction in s -waves is zero. The limit $\epsilon_{AA} \rightarrow 0$ is thus the relevant one for identical fermions in the zero-range model employed here. We note that this ignores interactions between the fermions in the p -wave channel which are usually always negligible in comparison to the interactions in the s -wave channel between non-identical A and B particles.

Using mass unit $m_A = 1$ and choosing the binding energy $|E_{AB}| = 1$, which is equivalent to rescaling all momenta by $\mathbf{q}(\mathbf{k}) \rightarrow \sqrt{|E_{AB}|} \mathbf{q}(\mathbf{k})$ in the set of coupled homogeneous integral equations (10) and (11), one obtains

$$f_B(\mathbf{q}) = \left[\pi \ln \left(\sqrt{\frac{m+2}{4m} \mathbf{q}^2 + \epsilon_3} \right) \right]^{-1} \times \int d^2k \frac{f_A(\mathbf{k})}{\epsilon_3 + \frac{m+1}{2m} \mathbf{q}^2 + \mathbf{k}^2 + \mathbf{k} \cdot \mathbf{q}}, \quad (15)$$

$$f_A(\mathbf{q}) = \left[4\pi \frac{m}{m+1} \ln \left(\sqrt{\frac{m+2}{2(m+1)} \mathbf{q}^2 + \epsilon_3} \right) \right]^{-1} \times \left[\int d^2k \frac{f_B(\mathbf{k})}{\epsilon_3 + \mathbf{q}^2 + \frac{m+1}{2m} \mathbf{k}^2 + \mathbf{k} \cdot \mathbf{q}} + \int d^2k \frac{f_A(\mathbf{k})}{\epsilon_3 + \frac{m+1}{2m} (\mathbf{q}^2 + \mathbf{k}^2) + \frac{1}{m} \mathbf{k} \cdot \mathbf{q}} \right]. \quad (16)$$

The coupled integral equations, (15) and (16), give the scaled three-body energies, ϵ_3 as functions, $\mathcal{F}_n(\epsilon_{AA}, m)$, of the two independent parameters. We emphasize that E_{AA} , E_{AB} , and E_3 are binding energies while ϵ_3 and ϵ_{AA} are ratios of binding energies and will be referred to as scaled three- and two-body energy, respectively. An analytical solution is not available and we shall instead investigate the functions \mathcal{F}_n by numerical means. We first concentrate on \mathcal{F}_0 and its dependence on energy and mass.

3.1. Dependence on two-body energy

The solutions are firmly established for the completely symmetric case of $\epsilon_{AA} = 1$ and $m = 1$, where all masses are equal and all pairs have the same binding energy. Then

two, and only two, bound three-body states exist with energies given by [1, 2, 3, 27]

$$\epsilon_3^{(0)} = 16.52 \text{ and } \epsilon_3^{(1)} = 1.27, \quad (17)$$

where the superscript denote ground and first excited state, respectively. These results have been confirmed by several studies using different numerical techniques [55, 56, 57, 58]. The two-body binding energies are $E_{AB} = E_{AA} = E_2 = -4\hbar^2/(\mu a^2) \exp(-2\gamma)$, where a is the scattering length, μ is the two-body reduced mass and $\gamma = 0.57721$ is Euler's constant.

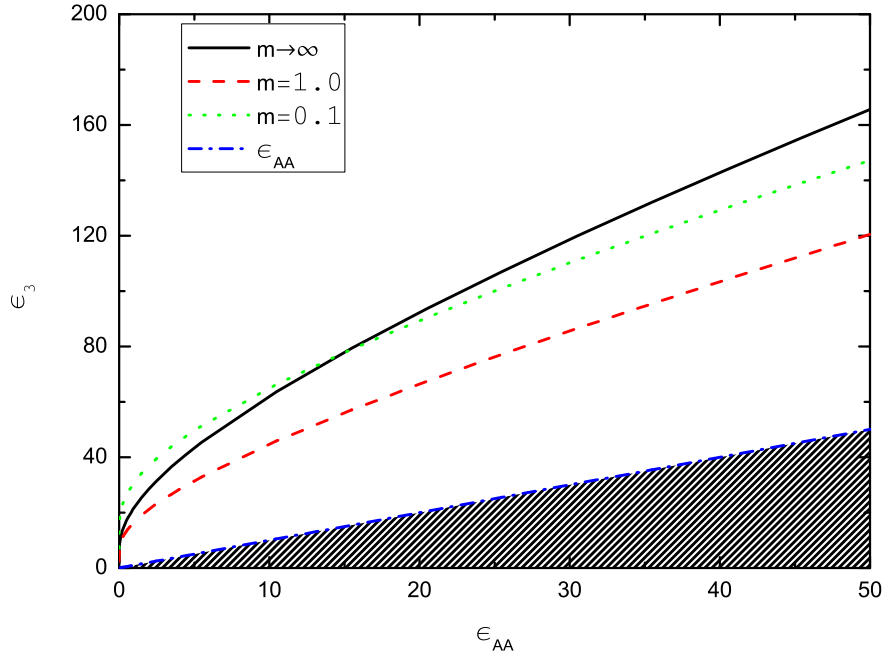


Figure 2. Scaled three-body binding energy, $\epsilon_3 = \mathcal{F}_0(\epsilon_{AA}, m)$, as function of the scaled two-body energy (ϵ_{AA}) for the ground state with $m = 0.1$, $m = 1.0$, and $m \rightarrow \infty$. States with energies above the $\epsilon_3 = \epsilon_{AA}$ line are stable. The highest-lying curve for large ϵ_{AA} corresponding to infinite mass is the function $\mathcal{A}_0(\epsilon_{AA})$ in (22). The curves for all other values of m are located between the $m = 1$ and $m \rightarrow \infty$ lines in the asymptotic region ($\epsilon_{AA} \gtrsim 15$).

For the ground state, the scaled three-body energies are shown in figure 2 as function of the scaled two-body energy, ϵ_{AA} , for several mass ratios, m . The curve for $m = 1$ must go through the point $(1.0, 16.52)$ corresponding to three identical bosons. The straight line, $\epsilon_3 = \epsilon_{AA}$, is inserted to show that the three-body system has a stable ground state with binding energy larger than that of the subsystems. Equivalently, for the binding energies we have $E_3 < E_2$, where E_2 is the smallest of the two-body binding energies E_{AB} and E_{AA} (below we will use the notation $\epsilon_2 = E_2/E_{AB}$ for the corresponding scaled quantity). A finite number of stable excited states may also exist with energies above the $\epsilon_3 = \epsilon_{AA}$ line.

All curves in figure 2 increase rather steeply from $\epsilon_{AA} = 0$ where ϵ_3 must be finite since the binding energy of the two pairs of particles, E_{AB} , is finite. The behavior of

Table 1. Values of $\mathcal{G}_1(m)$ for $m = 0.1, 1.0$ and 10.0 .

$\mathcal{G}_1(0.1)$	$\simeq 4657$
$\mathcal{G}_1(1.0)$	$\simeq 5751$
$\mathcal{G}_1(10.0)$	$\simeq 12332$

the curves for small ϵ_{AA} is found to be

$$\epsilon_3 = \mathcal{F}_0(\epsilon_{AA}, m) = \mathcal{F}_0(0, m)(1 + \mathcal{G}_0(\epsilon_{AA})), \text{ for } \epsilon_{AA} \rightarrow 0, \quad (18)$$

where $\mathcal{F}_0(0, m)$ is a function of mass, and $\mathcal{G}_0(\epsilon_{AA})$ is a function of energy with $\mathcal{G}_0(\epsilon_{AA} = 0) = 0$ and a very large derivative at $\epsilon_{AA} = 0$, like for example $\mathcal{G}_0(x) \propto x^s$ with s less than 1. The limit $\epsilon_{AA} \rightarrow 0$ applies to two identical fermions. The singular behavior of the energy in this weak-coupling limit is also found in many-body studies of 2D bosonic systems [59, 60] and in two-component 2D Fermi gases [61, 62].

The curves in figure 2 all increase almost linearly with ϵ_{AA} for large ϵ_{AA} . The deviation from linearity is very well approximated by a logarithmic modification factor, i.e.

$$\epsilon_3 = \mathcal{F}_0(\epsilon_{AA}, m) \approx \epsilon_{AA} \ln \left(\frac{\mathcal{G}_1(m)}{\epsilon_{AA}} + e \right), \text{ for } \epsilon_{AA} \rightarrow \infty, \quad (19)$$

where $\mathcal{G}_1(m)$ is an increasing function of m as seen from the values given in table 1. In the extreme limit, we have $\epsilon_3 \rightarrow \epsilon_{AA}$. Here the system is simply that of an AA molecule with binding energy E_{AA} and a single B particle with a negligible contribution to the energy.

As the scaled two-body energy ϵ_{AA} increases, the two strongly interacting particles contract into one tightly bound dimer entity for all m . In the limit $\epsilon_{AA} \rightarrow \infty$ we are thus left with a two-body problem effectively. It is known that for any two-body system in 2D we always have a bound state [10], which is the ground state found here. The three-body binding energy in the limit where $|E_{AA}| \gg |E_{AB}|$, or $\epsilon_{AA} \gg 1$, is expected to be approximately the two-body binding energy between the two identical bosons. The other contributions become of much less importance and give a weak logarithmic energy dependence. All these features are present in the asymptotic parametrization in (19).

The lines in figure 2 all have qualitatively the same shape. However, sometimes they cross each other. This behavior is better appreciated in figure 3 where a much larger variation of ϵ_{AA} is shown. When $\epsilon_{AA} \ll 1$, we see that the three-body energy increases with decreasing mass ratio, whereas the three-body energy increases with increasing mass ratio for $\epsilon_{AA} \gg 1$. This feature of figures 2 and 3 is also easily seen in figure 4 below. The limit of $\epsilon_{AA} \rightarrow 0$ on figure 4 agrees well with the calculation of one fermion and two bosons with resonant boson-fermion interaction given in [57].

3.2. Mass dependence

The mass dependence of \mathcal{F}_0 is shown in figure 4 for the ground state for several values of ϵ_{AA} . When m becomes large, the system consists of one heavy and two light particles.

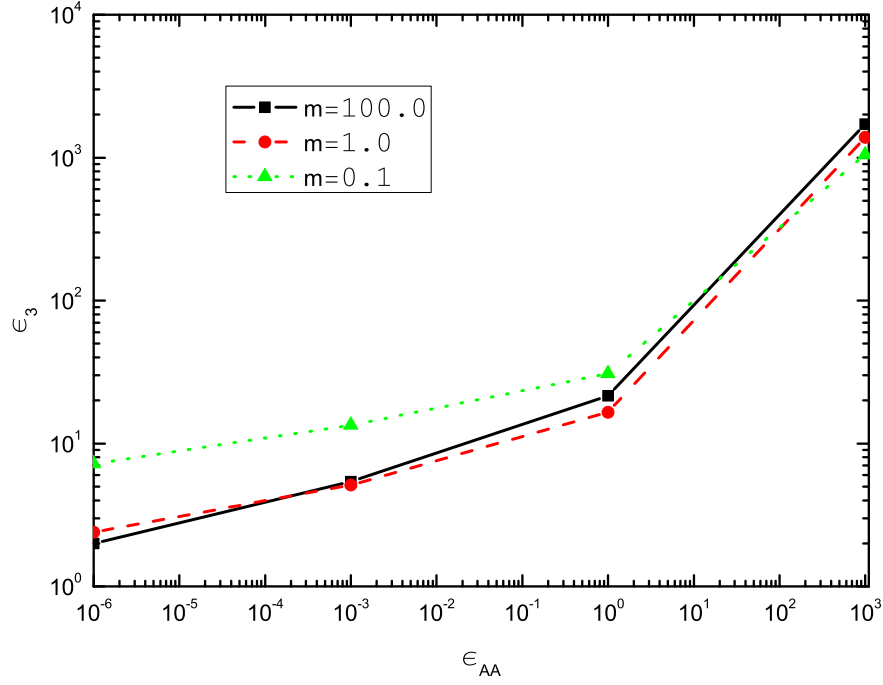


Figure 3. Scaled three-body ground state energy $\epsilon_3 = \mathcal{F}_0(\epsilon_{AA}, m)$ for large variations of ϵ_{AA} with $m = 0.10$, $m = 1.0$, and $m = 100$.

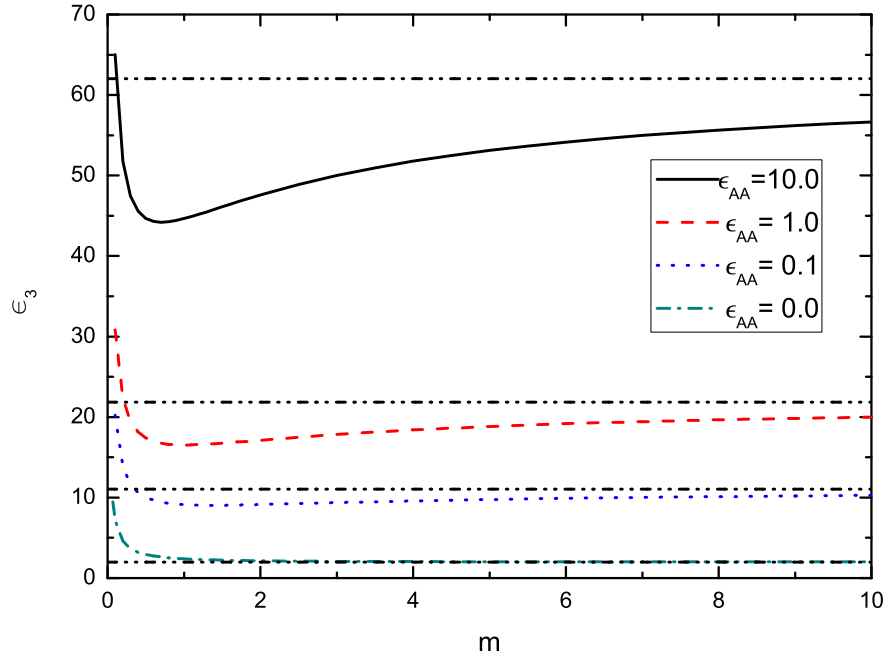


Figure 4. The scaled three-body ground state energy, $\epsilon_3 = \mathcal{F}_0(\epsilon_{AA}, m)$, as function of mass ratio, m , for $\epsilon_{AA} = 0$, $\epsilon_{AA} = 0.1$, $\epsilon_{AA} = 1$, and $\epsilon_{AA} = 10$. The dash-dot-dotted lines show the asymptotic large- m values.

By rewriting (15) and (16) for arbitrary ϵ_{AA} in the limit of large m , we obtain mass

independent equations, i.e.

$$f_B(\mathbf{q}) = \left[\pi \ln \left(\sqrt{\frac{\frac{1}{4}\mathbf{q}^2 + \epsilon_3}{\epsilon_{AA}}} \right) \right]^{-1} \int d^2k \frac{f_A(\mathbf{k})}{\epsilon_3 + \frac{1}{2}\mathbf{q}^2 - \mathbf{k}^2 - \mathbf{k} \cdot \mathbf{q}}, \quad (20)$$

$$f_A(\mathbf{q}) = \left[4\pi \ln \left(\sqrt{\frac{1}{2}\mathbf{q}^2 + \epsilon_3} \right) \right]^{-1} \left[\int d^2k \frac{f_B(\mathbf{k})}{\epsilon_3 + \mathbf{q}^2 - \frac{1}{2}\mathbf{k}^2 - \mathbf{k} \cdot \mathbf{q}} + \int d^2k \frac{f_A(\mathbf{k})}{\epsilon_3 + \frac{1}{2}(\mathbf{q}^2 + \mathbf{k}^2)} \right]. \quad (21)$$

Thus, for large values of m the scaled three-body energy becomes m -independent and approaches an energy-dependent constant as seen in figure 4. The limit can be expressed as

$$\epsilon_3 = \mathcal{F}_0(\epsilon_{AA}, m) \rightarrow \mathcal{F}_0(\epsilon_{AA}, \infty), \text{ for } m \rightarrow \infty, \quad (22)$$

where $\mathcal{F}_0(\epsilon_{AA}, \infty)$ is the $m \rightarrow \infty$ line shown in figure 2. The high-energy behavior is related to (19) where $\mathcal{F}_0(\epsilon_{AA}, \infty)$ is obtained from $\mathcal{G}_1(m = \infty)$. The curve $\mathcal{F}_0(0, \infty)$ approaches the structure of two mutually non-interacting light particles each interacting with the same heavy particle. The total energy is therefore a sum of the two light-heavy particle energies, that is a total energy of $2E_{AB}$, as seen for large m and $\epsilon_{AA} = 0$ in figure 4. This can also be considered an accuracy test of the numerical procedure.

Decreasing the mass ratio towards zero leads to an increasing scaled three-body energy which rises rather quickly when m becomes smaller than about 0.2, as seen in figure 4. In the limit of vanishing m , where the system consists of one light and two heavy particles, all three-body energies diverge. This is found from the diverging terms in (15) and (16), which are compensated by a diverging three-body energy. Furthermore, infinitely many bound states simultaneously appear. This behavior can be studied in the Born-Oppenheimer approximation, where a screened Coulomb-like energy behavior emerges [63] in the limit of vanishing mass ratio m . This can be seen in the next section in figure 6, where we find that $\epsilon_3 \propto \frac{1}{m}$ for $m \rightarrow 0$ when $\epsilon_{AA} = 0$, that is

$$\epsilon_3 = \mathcal{F}_n(0, m) \rightarrow \mathcal{B}_n \frac{1}{m}, \text{ for } m \rightarrow 0, \quad (23)$$

where \mathcal{B}_n is a constant depending on whether ground or excited state is considered.

Through inspection of figures 2 and 4 we realize that the minimum possible scaled three-body energy is found in the limits $\epsilon_{AA} \rightarrow 0$ and $m \rightarrow \infty$. Correspondingly we realize that the maximum scaled three-body energy is found in the limits $\epsilon_{AA} \gg 1$ and $m \rightarrow \infty$. Actually the three-body energy diverges for small m , so this maximum is found only if we exclude the very small m region.

The crossing behavior in figures 2, 3, and 4 can be related to the mass dependence of ϵ_3 . Let us focus on two vertical lines in figure 4 for mass ratios $m = 0.1$ and $m = 10$. We notice that $\mathcal{F}_0(0, 0.1) > \mathcal{F}_0(0, 10)$ and $\mathcal{F}_0(10, 0.1) < \mathcal{F}_0(10, 10)$. Therefore there must exist a scaled energy, ϵ_{AA} , such that $\mathcal{F}_0(\epsilon_{AA}, 0.1) = \mathcal{F}_0(\epsilon_{AA}, 10)$, corresponding to the point of crossing. The same procedure can be followed for all the possible crossing points.

4. Stability

Stability of the pure three-body system is determined by the scaled energy ϵ_3 compared to the thresholds for binding two of the constituent particles. This means that if the scaled energy ϵ_3 is larger than all thresholds the three-body system is stable. This suggests to measure the excess of ϵ_3 over the largest scaled two-body energy, that is ϵ_{AA} or 1, when ϵ_{AA} is larger or smaller than 1, respectively. For $\epsilon_{AA} \geq 1$ the threshold is increasing with ϵ_{AA} , and for $\epsilon_{AA} \leq 1$ the threshold is $|E_{AB}|$ which in our units is equal to 1.

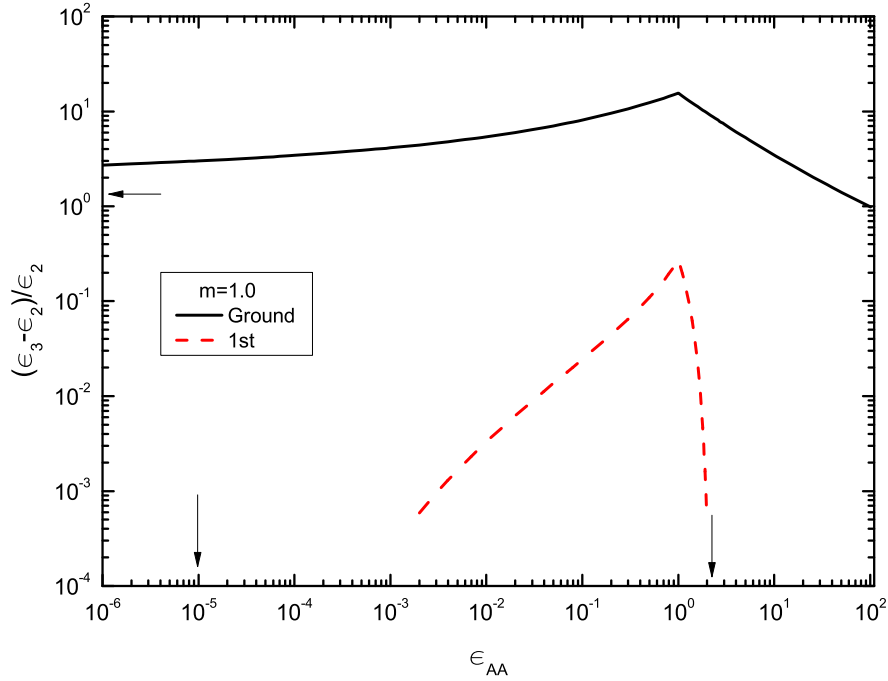


Figure 5. The relative three-body energy, $(\epsilon_3 - \epsilon_2)/\epsilon_2$, of ground and first excited states for $m = 1$ as function of scaled two-body energy ϵ_{AA} . We show the scaled three-body energy relative to the possible thresholds, ϵ_2 , of binding the two two-body subsystems. Here ϵ_2 is the largest value of ϵ_{AA} and 1. For $\epsilon_{AA} \leq 1$ the threshold is 1 and for $\epsilon_{AA} \geq 1$ the threshold is ϵ_{AA} . The peaks result from the different thresholds. The solid (black) and dashed (red) lines refer to ground and excited states, respectively. The \downarrow arrow indicates the points given in table 3, while the \leftarrow indicates the $\epsilon_{AA} = 0$ limit.

4.1. Identical masses

Consider first $m = 1$ where we already know that two three-body bound states exist for three identical bosons. We show in figure 5 the stability plot for both ground and first excited states. Stability for both states corresponds to positive values of $\epsilon_3 > \epsilon_{AA} \geq 1$, and values larger than 1 for $\epsilon_{AA} \leq 1$. We observe the known ground state stability for all scaled two-body energies, ϵ_{AA} . The peaks are an artifact of plotting relative to different thresholds.

We see in figure 5 how both these states move with respect to the threshold of stability. The variation is so large that we need to use log-log scales. For $\epsilon_{AA} = 1$ we find the values in (17), that is 16.52 and 1.27 for ground and excited state, respectively. The ground state remains above the thresholds for all values of ϵ_{AA} . However, the excited state approaches the threshold of stability for both large and small ϵ_{AA} , that is one excited state is present for $m = 1$ only when the underlying two-body energies are in the interval, $1.00 \times 10^{-5} \leq \epsilon_{AA} \leq 2.36$. This is detailed in table 3 for three different mass ratios.

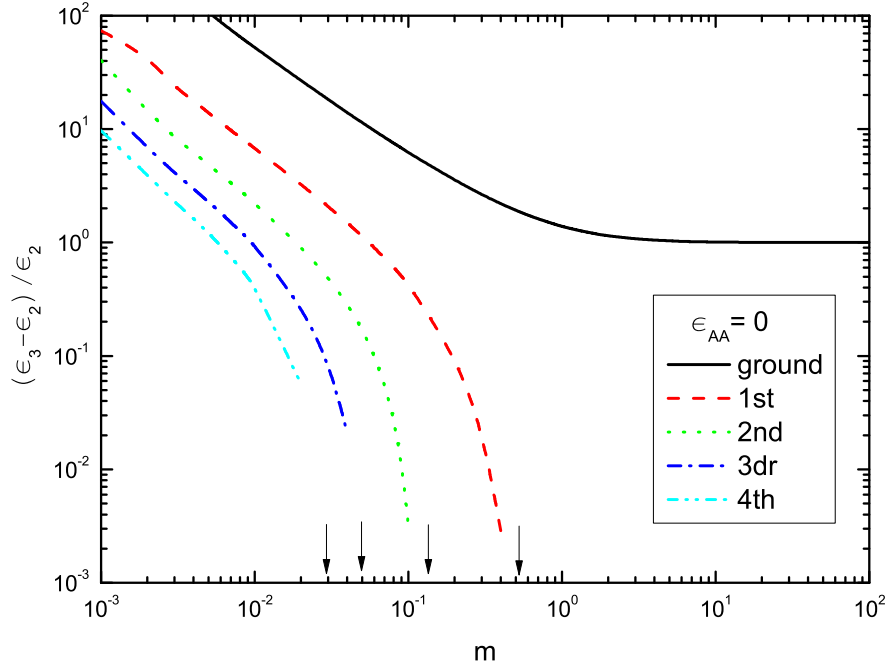


Figure 6. The relative three-body energies, $(\epsilon_3 - \epsilon_2)/\epsilon_2$, for $\epsilon_{AA} = 0$ as function of m . The \downarrow arrows indicate the m -values where the states successively emerge ($\epsilon_3 = \epsilon_2$). When $m \rightarrow \infty$ we have $\epsilon_3 \rightarrow 2\epsilon_2$.

For non-identical particles with different interactions and masses, the number of stable bound states may be completely different. The conditions for existence of excited states can be formulated much more conveniently for different values of m . In general, the three-body binding energy of any excited state has to be smaller than the smallest threshold for binding any subsystem. In figure 6 we see that for $\epsilon_{AA} = 0$ (directly applicable for identical fermions) and $m = 1$ only the ground state is bound. This means that the excited state appears for $\epsilon_{AA} = 0$ when ϵ_3 exceeds the threshold of 1, and ceases to exist for $\epsilon_3 = \epsilon_{AA}$ when $\epsilon_{AA} > 1$. These conditions refer to the different thresholds, ϵ_{AA} and 1, for $\epsilon_{AA} > 1$ and $\epsilon_{AA} < 1$, respectively.

We can introduce the threshold condition, $\epsilon_{AA} = 0$, in (15) and (16). The result is that only one equation remains, i.e.

$$f_A(\mathbf{q}) = \left[4\pi \frac{m}{m+1} \ln \left(\sqrt{\frac{m+2}{2(m+1)}} \mathbf{q}^2 + \epsilon_3 \right) \right]^{-1} \times$$

Table 2. The mass ratio threshold, m_t , for appearance of stable excited states as the mass ratio decrease towards zero for $\epsilon_{AA} = 0$.

1st	$m_t \simeq 0.55$
2nd	$m_t \simeq 0.12$
3rd	$m_t \simeq 0.05$
4th	$m_t \simeq 0.03$

$$\int d^2k \frac{f_A(\mathbf{k})}{\epsilon_3 + \frac{m+1}{2m}(\mathbf{q}^2 + \mathbf{k}^2) + \frac{1}{m}\mathbf{k} \cdot \mathbf{q}}. \quad (24)$$

This means that the two identical particles in the limit of vanishing energy, $\epsilon_{AA} = 0$, do not feel each other and the distinct particle only feel the potential separately from one or the other. This holds for trivially for identical bosons, and for identical fermions since we have neglected higher partial waves in the interaction.

4.2. Excited states

A survey of the results are shown in figure 6 as function of m . The ground state is always stable and approaches 2 as $m \rightarrow \infty$. The excited states appear one after the other as m decreases from $m = 1$ towards zero where the system consists of two heavy and one light particle. From 3D physics we are very familiar with this behavior of a denser spectrum for such a system. Ultimately, infinitely many stable bound states exist in the limit of $m = 0$.

The log-log plot is necessary in figure 6 for the general overview but does not expose the precise value of m at the thresholds for the appearance which is defined by a positive value in figure 6. These thresholds are instead indicated by arrows and more precise values of the mass ratios are given in table 2. We note in both table and figure how the excited states appear closer to each other as $m \rightarrow 0$.

We now investigate how these results vary as function of ϵ_{AA} and m . We know from figure 6 that for $m = 10$ or $m = 0.1$ we have only one or three bound states, respectively. An interesting question is for which value of ϵ_{AA} will the number of bound states change when we keep m fixed. The results are shown in figure 7 for $m = 10$ and $m = 0.1$. Again the precise thresholds cannot be seen in this figure, and we present therefore the values in table 3. We see that for $m = 10$ only the ground and first excited state are stable, while for $m = 0.1$ the second excited state is also found to be stable.

From figures 6 and 7, and from table 3 the question arises of how low m should be before the next excited state appears. The condition is that the three-body energy ϵ_3 has to exceed both ϵ_{AA} and 1. In other words, the thresholds where the state begins and ceases to exist are equal. Therefore we search for the m values where solutions to (15) and (16) exist for which ϵ_3 equals the threshold values of ϵ_{AA} and 1. We conclude that both ground and first excited states always exist for any value of m , provided the two-body energy ϵ_{AA} assumes an appropriate value depending on m , as we now explain.

A higher number of excited states only exists if the mass ratio m is sufficiently

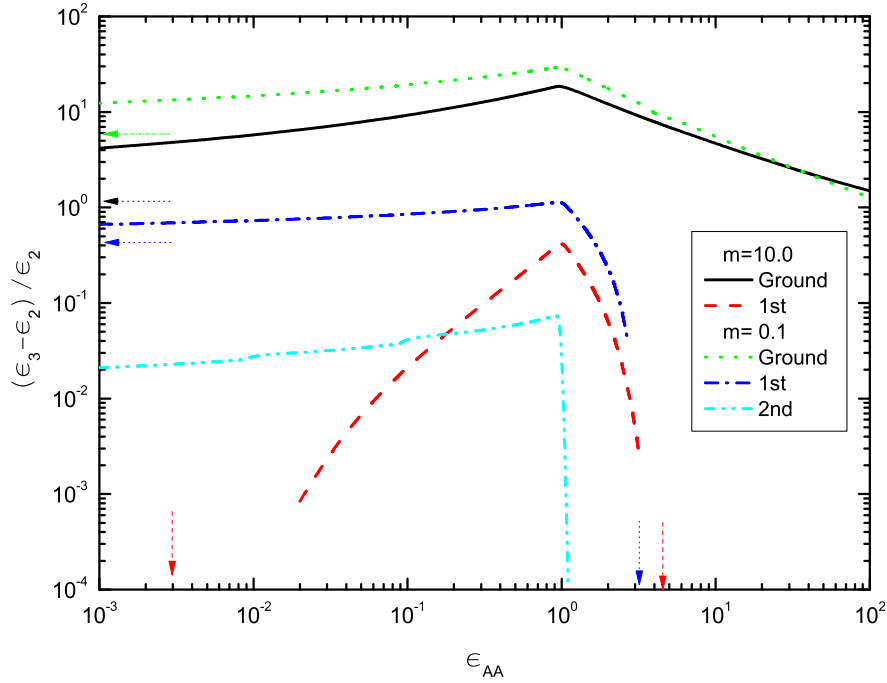


Figure 7. The relative three-body energy, $(\epsilon_3 - \epsilon_2)/\epsilon_2$ of ground and first excited states for $m = 0.1$ and $m = 10$ as function of the scaled two-body energy ϵ_{AA} . Here ϵ_2 is the largest value of ϵ_{AA} and 1. For $\epsilon_{AA} \leq 1$ the threshold is 1 and for $\epsilon_{AA} \geq 1$ the threshold is ϵ_{AA} . The peaks result from the different thresholds. Solid (black) and dashed (red) lines are ground and first excited states, respectively, for $m = 10$. Dotted (green), dash-dotted (blue) and dash-double dotted (cyan) lines are ground, first, and second states, respectively, for $m = 0.1$. The \downarrow arrows mark the thresholds given in table 3. The \leftarrow arrows indicate the $\epsilon_{AA} = 0$ limit.

Table 3. The energy intervals for appearance of stable excited states for different mass ratios m .

State	m	ϵ_{AA}^{\min}	ϵ_{AA}^{\max}
gr.	0.1	0.0	∞
	1	0.0	∞
	10	0.0	∞
1st	0.1	0.0	3.76
	1	1.10×10^{-5}	2.36
	10	3.00×10^{-3}	4.69
2nd	0.1	0.0	1.08
	1	—	—
	10	—	—

small. For example if $m \geq 0.22$ only ground and first excited states can be present. We give in table 4 the critical masses for appearance of a higher number of bound states. These critical masses are indicated with arrows in figure 8 where we show the $m - \epsilon_{AA}$ phase diagram for the number of stable excited states. As an example of the use of

Table 4. The critical mass ratios, m_c , above which only N_c bound states can exist.

N_c	m_c
2	0.22
3	0.07
4	0.04
5	0.02

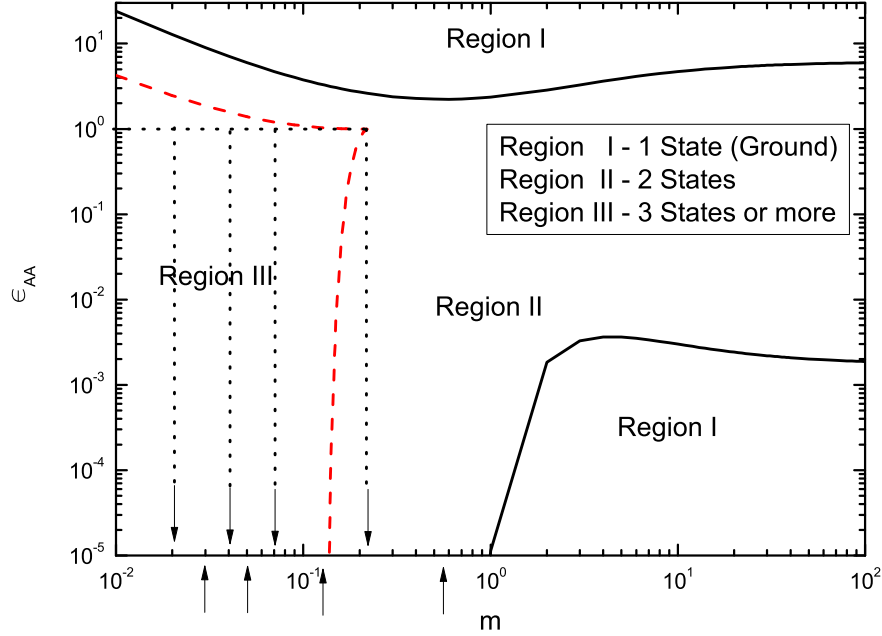
**Figure 8.** The $m - \epsilon_{AA}$ contour diagram of regions where stable excited three-body states exist. In Region I only the ground state is stable. In Region II the ground and the first states are both stable. In Region III three or more states are stable. The solid (black) and dashed (red) lines show the limits where the first and second excited states are stable. The \downarrow arrows mark the critical masses, (m_c), for which the next excited state appears, table 4. The \uparrow arrows indicate the masses for which the next excited state emerges when $\epsilon_2 = 0$, table 2.

figure 8, we can conclude that at most ground and first excited state are present for $m = 1$ and $m = 10$, whereas no more than three bound states exist for $m = 0.1$. It is worth emphasizing that the critical mass for appearance of the third stable bound state is at the kink of the dashed (red) curve in the middle of figure 8. The threshold is not for $\epsilon_{AA} = 0$ as the almost vertical curve otherwise seems to indicate.

4.3. Realistic systems

The results in figure 8 may seem strange; the number of stable bound states decrease when one of the two-body attractions increase. This is similar to the number of Efimov states in a 3D system. If we start on the side of the resonance where no two-body bound state is present (negative scattering length, $a < 0$, in a typical zero-range model,

see for instance figure 1 in [20]) then the number of bound states is finite (and can be zero). When the attraction to the resonance ($|a| = \infty$) the number of states is infinite. On the other side of the resonance ($a \rightarrow 0^+$) the number of bound states will start to decrease again to a finite number. For the Efimov states the explanation is that, although all energies decrease with increasing attraction, the three-body states catch up with the two-body threshold [15]. The result is that three-body states disappear into the two-body continuum, and the number of bound states decreases as a consequence. In complete analogy, the energies of the present excited three-body bound states also decrease with increasing attraction. However, the two-body thresholds decrease faster, and the three-body states become unstable as they merge with the two-body continuum.

In general, figure 8 shows the number of bound states for any set of parameters (ϵ_{AA}, m) . This pair of numbers can be related to any set of two-body energies and masses through the scaling relation in (13) and (14). Thus for any given point in figure 8 we find the true three-body binding energy from figure 2. In the Regions I and II we have one and two stable states, respectively. Region III collects parameter intervals where more than two stable bound states are present. This region could be subdivided by a number of curves similar to the dashed (red) curve. Thresholds for $\epsilon_{AA} = 0$ are shown but finite values of ϵ_{AA} extend the mass regions as the boundary between regions II and III. We expect that $0.07 < m < 0.22$ allow up to three while $0.04 < m < 0.07$ allow up to four stable bound states. Better values are given in table 4.

Some commonly used alkali atoms for ultracold atomic experiments are ^6Li , ^{40}K , ^{87}Rb , and ^{133}Cs . These mass ratios range from 0.05 to 22. The pairwise interaction is usually tunable by Feshbach resonances. Therefore we have to look for variations of the dependence on the two-body binding energies. From figure 8 and table 4 we see that if $m \geq 0.22$ at most two bound states exist. Whether the first excited state is present or not depends on ϵ_{AA} . If $m < 1$ and ϵ_{AA} is larger than about 1, only the ground state is stable. If $m > 1$ and ϵ_{AA} is between about 0.001 and 1 also the first excited state is stable. When m is slightly less than 0.22 both 1, 2, and 3 stable states may be present depending on ϵ_{AA} . As m decreases below 0.22, an increasing number of stable states are possible when ϵ_{AA} is sufficiently small as indicated in figure 8.

The 2D structures are not yet routinely made but a number of experimental investigations on identical particles have been reported as discussed in the introduction. There we also pointed out some modifications expected from the fact that the experiments are only quasi-2D. If we consider a layered system with long-range interactions as shown in figure 1b) then particles can be placed in two or three equidistant layers. For example, if we consider three layers and place the identical particles in the outer layers and the distinct particle in the central layer, then the scaled two-body energy ϵ_{AA} is about 0.25 when all particles have the same mass, see e.g. [48, 64]. Precisely two bound states are present in the universal regime for this setup. This still holds when the mass ratio is larger than 1. However, when the mass ratio decreases, more excited states may be present.

The physics of highly polarized Fermi gases is also interesting in relation to the

present study. The problem of a single impurity interacting with a Fermi sea of particles in 2D has generated considerable theoretical interest recently [65, 66, 67]. Furthermore, fermionic impurities in Bose-Einstein condensates have recently been studied in experimentally in optical lattices (although so far only in 3D) [68]. Theoretical studies of these kinds of setups usually focus mostly on the influence of two-body bound states. However, we expect that interesting spectra of three-body states can occur in these systems and it will be interesting to study how a many-body background such as a Fermi sea or a condensate can affect the properties of three-body states.

5. Summary and conclusions

In the present paper we investigate the three-body problem in two dimensions. The aim is to extract universal properties where any potential with similar (observable) constraints is able to describe the model-independent results. This only occurs when the properties hinges on large-distance behaviour where the details of the basic two-body ingredients are unimportant. Zero-range models are then suitable since all properties are determined at distances outside the potential. We therefore employ the established method of solving the momentum-space Faddeev equations with zero-range interactions.

We focus for simplicity on a three-body system with two identical and one distinct particle. Three different particles would be essentially as easy to solve but the number of free parameters would be doubled and the results much harder to display and digest. We leave this generalization for a separate future investigation. We first establish that the three-body energy in units of one of the two-body binding energies E_{AB} must be a function of only two parameters; the ratio of the other two-body binding energy E_{AA} to E_{AB} , and the mass ratio $m = m_B/m_A$. We investigate this two-parameter problem as function of the reduced energy and mass parameters. When the identical particles are fermions their binding energy is zero in the zero-range model, i.e. $E_{AA} = 0$.

The starting point is three identical bosons where the energies of the two stable bound states are well-known. The scaled three-body energy is calculated as function of the scaled two-body energy for fixed mass ratio and vice versa. The energy dependence is the stronger than the mass dependence and always monotonically increasing, and we establish logarithmic dependence of the scaled three-body energy for large two-body energy. The mass dependence for fixed scaled two-body energy is in general smaller but non-monotonic. It is divergently increasing when the mass ratio approaches zero, while an energy-dependent and mass-independent constant is approached for large mass ratios.

A number of excited stable bound states can exist. In general when two equal masses are not large compared to the third, ground and first excited states exist and are stable. These two lowest states are always possible for all mass ratios but, whenever the mass ratio is outside the interval $0.22 < m < 1$, the first excited state only occurs for a rather narrow band of two-body energies. As the two equal masses become heavier the number of stable bound states increase towards infinity. This happens when the mass

ratio approaches zero and corresponds to the Born-Oppenheimer limit. We derive a number of threshold values of masses and energies for appearance of these stable excited states. Finally, we provide an energy-mass phase-diagram of regions for occurrence of specific numbers of excited states and discuss applications for realistic systems.

In conclusion, we have established the two-dimensional universal energy relations for a three-body system of two identical and one distinct particle. These investigations are of interest as properties of basic quantum mechanical problems extended to two dimensions where the behavior differ qualitatively from that of three dimensions. We furthermore expect that our results will become directly relevant in the topical studies of two-dimensional systems in cold atomic gases.

Acknowledgments

This work was partly support by funds provided by Fundação de Amparo à Pesquisa do Estado de São Paulo and Conselho Nacional de Desenvolvimento Científico e Tecnológico (Brazil). FFB, MTY and TF thanks the hospitality of the Department of Physics and Astronomy of Aarhus University during their visits.

- [1] Nielsen E, Fedorov D V and Jensen A S 1997 *Phys. Rev. A* **56** 3287
- [2] Nielsen E, Fedorov D V and Jensen A S 1999 *Few-body Syst.* **27** 15
- [3] Nielsen E, Fedorov D V, Jensen A S and Garrido E 2001 *Phys. Rep.* **347** 373
- [4] Landau L D and Lifshitz E M 1977 *Quantum Mechanics* (Pergamon Press, Oxford)
- [5] Simon B 1976 *Ann. Phys.* **97** 279
- [6] Armstrong J R, Zinner N T, Fedorov D V and Jensen A S 2010 *Europhys. Lett.* **91** 16001
- [7] Klawunn M, Piovski A and Santos L 2010 *Phys. Rev. A* **82** 044701
- [8] Baranov M A, Micheli A, Ronen S and Zoller P 2011 *Phys. Rev. A* **83** 043602
- [9] Volosniev A G, N T Zinner, Fedorov D V, Jensen A S and Wunsch B 2011 *J. Phys. B: At. Mol. Opt. Phys.* **45** 125301
- [10] Volosniev A G, Fedorov D V, Jensen A S and Zinner N T 2011 *Phys. Rev. Lett.* **106** 250401
- [11] Efimov V 1970 *Yad. Fiz* **12** 1080; 1970 *Sov. J. Nucl. Phys.* **12** 589
- [12] Phillips A C 1968 *Nucl. Phys. A* **107** 209
- [13] Coester F, Day B, Goodman A 1970 *Phys. Rev. C* **1** 769
- [14] Tjon J A 1975 *Phys. Lett. B* **56** 217
- [15] Jensen A S, Riisager K, Fedorov D V and Garrido E 2004 *Rev. Mod. Phys.* **76** 215
- [16] Nielsen E, Fedorov D V and Jensen A S 1998 *J. Phys. B: At. Mol. Opt. Phys.* **31** 4085
- [17] Amorim A E A, Frederico T and Tomio L 1997 *Phys. Rev. C* **56** R2378
- [18] Delfino A, Frederico T and Tomio L 2000 *J. Chem. Phys.* **113** 7874
- [19] Kraemer T *et al.* 2006 *Nature* **440** 315
- [20] Ferlaino F and Grimm R 2011 *Physics* **3** 9
- [21] Barontini G *et al.* 2009 *Phys. Rev. Lett.* **103** 043201
- [22] Platter L, Hammer H and Meißner U 2004 *Phys. Rev. A* **70** 52101
- [23] Yamashita M T, Tomio L, Delfino A and Frederico T 2006 *Europhys. Lett.* **75** 555
- [24] von Stecher J, D'Incao J P and Greene C H 2009 *Nature Phys.* **5** 417
- [25] Pollack S E, Dries D and Hulet R G 2009 *Science* **326** 1683
- [26] Ferlaino F *et al.* 2009 *Phys. Rev. Lett.* **102** 140401
- [27] Bruch L W and Tjon J A 1979 *Phys. Rev. A* **19** 425
- [28] Randeria M, Duan J-M and Shieh L-Y 1989 *Phys. Rev. Lett.* **62** 981
- [29] Schmitt-Rink S, Varma C M and Ruckenstein A E 1989 *Phys. Rev. Lett.* **63** 445
- [30] Dreschler M and Zwerger W 1992 *Ann. Phys. (Leipzig)* **1** 15

- [31] Vuletić V, Chin C, Kerman A J and Chu S 1998 *Phys. Rev. Lett.* **81** 5768;
- [32] Morinaga M, Bouchoule I, Karam J-C and Salomon C 1999 *Phys. Rev. Lett.* **83** 4037
- [33] Hammes M, Rychtarik D, Engeser B, Nägerl H C and Grimm R 2003 *Phys. Rev. Lett.* **90** 173001
- [34] Görlitz A *et al.* 2001 *Phys. Rev. Lett.* **87** 130402
- [35] Bürger S *et al.* 2002 *Europhys. Lett.* **57** 1
- [36] Modugno G, Ferlaino F, Heidemann R, Roati G and Inguscio M 2003 *Phys. Rev. A* **68** 011601(R)
- [37] Günter K, Stöferle T, Moritz H, Köhl M and Esslinger T 2005 *Phys. Rev. Lett.* **95** 230401
- [38] Martiyanov K, Makhalov V and Turlapov A 2010 *Phys. Rev. Lett.* **105** 030404
- [39] Dyke P, Kuhnle E D, Whitlock S, Hu H, Mark M, Hoinka S, Lingham S, Hannaford P and Vale C J 2011 *Phys. Rev. Lett.* **106** 105304
- [40] Fröhlich B, Feld M, Vogt E, Koschorreck M, Zwerger W and Köhl M 2011 *Phys. Rev. Lett.* **106** 105301
- [41] de Miranda M G H *et al.* 2011 *Nature Phys.* **7** 502
- [42] Bloch I, Dalibard J and Zwerger W 2008 *Rev. Mod. Phys.* **80** 885
- [43] Haller E *et al.* 2010 *Phys. Rev. Lett.* **104** 153203
- [44] Lompe T, Ottenstein T B, Serwane F, Wenz A N, Zürn G and Jochim S 2010 *Science* **330** 940
- [45] Nakajima S, Horikoshi M, Mukaiyama T, Naidon P and Ueda M 2011 *Phys. Rev. Lett.* **106** 143201
- [46] Wunsch B, Zinner N T, Mekhov I B, Huang S-J, Wang D-W and Demler E 2011 *Phys. Rev. Lett.* **107** 073201
- [47] Wang Y, D’Incao J P and Greene C H 2011 *Phys. Rev. Lett.* **106** 233201
- [48] Armstrong J R, Zinner N T, Fedorov D V and Jensen A S 2011 *Preprint* arXiv:1106.2102v1
- [49] Frederico T, Tomio L, Delfino A, Hadizadeh M R and Yamashita M T, 2011 *Few-Body Syst.*, at press. (doi:10.1007/s00601-011-0236-7)
- [50] Adhikari S K, Delfino A, Frederico T, Goldman I D and Tomio L 1988 *Phys. Rev. A* **37** 3666
- [51] Adhikari S K, Delfino A, Frederico T and Tomio L 1993 *Phys. Rev. A* **47** 1093
- [52] Verhaar B J, de Goey L P H, van den Eijnde J P H W and Vredenburg E J D 1985 *Phys. Rev. A* **32** 1424
- [53] Adhikari S K and Frederico T 1995 *Phys. Rev. Lett.* **74** 4572
- [54] Helfrich K and Hammer H-W 2011 *Phys. Rev. A* **83** 052703
- [55] Hammer H-W and Son D T 2004 *Phys. Rev. Lett.* **93** 250408
- [56] Blume D 2005 *Phys. Rev. B* **72** 094510
- [57] Brodsky I V, Kagan M Yu, Klaptsov A V, Combescot R and Leyronas Y 2006 *Phys. Rev. A* **73** 032724
- [58] Kartavtsev O I and Malykh A V 2006 *Phys. Rev. A* **74** 042506
- [59] Schick M 1971 *Phys. Rev. A* **3** 1067
- [60] Lieb E H and Yngvason J 2001 *Jour. Stat. Phys.* **103** 509
- [61] Bloom P 1975 *Phys. Rev. B* **12** 125
- [62] Randeria M, Duan J-M and Shieh L-Y 1990 *Phys. Rev. B* **41** 327
- [63] Belotti F F *et al.*, in preparation
- [64] Armstrong J R, Zinner N T, Fedorov D V and Jensen A S 2011 *J. Phys. B: At. Mol. Opt. Phys.* **44** 055303
- [65] Zöllner S, Bruun G M and Pethick C J 2011 *Phys. Rev. A* **83** 021603(R)
- [66] Parish M M 2011 *Phys. Rev. A* **83** 051603(R)
- [67] Klawunn M and Recati A 2011 *Preprint* arXiv:1105.3431v1
- [68] Will S, Best T, Braun S, Schneider U and Bloch I 2011 *Phys. Rev. Lett.* **106** 115305